

28-8-2005

Shift estimation method based fringe pattern profilometry and performance comparison

Y. Hu

University of Wollongong, yingsong@uow.edu.au

Jiangtao Xi

University of Wollongong, jiangtao@uow.edu.au

Enbang Li

University of Wollongong, enbang@uow.edu.au

Joe F. Chicharo

University of Wollongong, chicharo@uow.edu.au

Zongkai Yang

Huazhong University of Science & Technology, China

Follow this and additional works at: <https://ro.uow.edu.au/infopapers>



Part of the [Physical Sciences and Mathematics Commons](#)

Recommended Citation

Hu, Y.; Xi, Jiangtao; Li, Enbang; Chicharo, Joe F.; and Yang, Zongkai: Shift estimation method based fringe pattern profilometry and performance comparison 2005.
<https://ro.uow.edu.au/infopapers/245>

Shift estimation method based fringe pattern profilometry and performance comparison

Abstract

In this paper, we present and study two approaches to fringe pattern profilometry (FPP) technique. Based on generalized analysis model for fringe pattern profilometry (FPP), Inverse Function based Shift Estimation (IFSE) and Gradient-based Shift Estimation (GSE) are proposed to calculate the shift between the projected and deformed fringe patterns. Further, computer simulations are utilized to compare the performance between these two methods. Meanwhile, we also compare these two algorithms with Phase Shift profilometry (PSP). It can be seen that both of these two shift estimation algorithms can significantly improve the measurement accuracy when the fringe patterns are nonlinearly distorted.

Disciplines

Physical Sciences and Mathematics

Publication Details

This article was originally published as: Hu, Y, Xi, J, Li, E, Chicharo, J & Yang, Z, Shift estimation method based fringe pattern profilometry and performance comparison, Proceedings of the Eighth International Symposium on Signal Processing and Its Applications, 28-31 August 2005, 2, 863-866. Copyright IEEE 2005.

SHIFT ESTIMATION METHOD BASED FRINGE PATTERN PROFILOMETRY AND PERFORMANCE COMPARISON

Yingsong Hu^{1,2}, Jiangtao Xi¹, Enbang Li¹, Joe Chicharo¹ and Zongkai Yang²

¹School of Electrical Computer and Telecommunications Engineering,
University of Wollongong, NSW 2522, Australia.

Department of Electronic and Information Engineering,

²Huazhong University of Science and Technology, Wuhan City, 430074, China

ABSTRACT

In this paper, we present and study two approaches to fringe pattern profilometry (FPP) technique. Based on generalized analysis model for fringe pattern profilometry (FPP), Inverse Function based Shift Estimation (IFSE) and Gradient-based Shift Estimation (GSE) are proposed to calculate the shift between the projected and deformed fringe patterns. Further, computer simulations are utilized to compare the performance between these two methods. Meanwhile, we also compare these two algorithms with Phase Shift profilometry (PSP). It can be seen that both of these two shift estimation algorithms can significantly improve the measurement accuracy when the fringe patterns are nonlinearly distorted.

1. INTRODUCTION

Fringe pattern profilometry (FPP) is one of the most popular non-contact methods for measuring the three dimensional surface of an object in recent years. With FPP, a Ronchi grating or sinusoidal grating is projected onto a three dimensional diffuse surface, the height distribution of which deforms the projected fringe patterns and modulates them in phase domain. Hence by retrieving the phase difference between the original and deformed fringe patterns, three dimensional profilometry can be achieved. A number of fringe pattern analysis methods have been developed for FPP, including Fourier Transform Profilometry (FTP)[1, 2], Phase Shifting Profilometry (PSP)[3], Spatial Phase Detection (SPD)[4], Phase Locked Loop[5] and other analysis methods[6, 7], all of which are based on an assumption that the projected fringe patterns are or can be filtered to be sinusoidal.

In recent years, because of the simplicity and controllability, digital projectors have been widely used to yield fringe patterns for implementing FPP[8, 9]. However, it is very difficult for projectors to produce pure sinusoidal fringe patterns due to the existence of geometrical distortion and colour distortion. Although digital filtering can be used to reduce the distortion, the resulting fringe patterns may still not be pure sinusoidal, as the digital filters are usually not ideal either. Additionally, when the deformed fringe pattern has an overlapped spectra, band-pass filtering will be unusable if a precise measurement

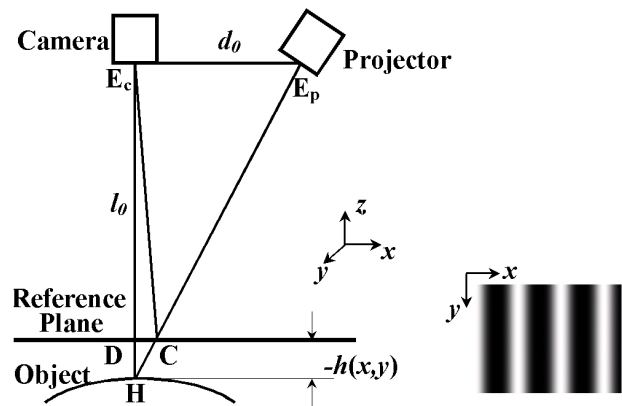


Fig. 1. Schematic diagram of fringe pattern profilometry (FPP) system

is required[1]. Therefore, errors will arise if the measurement is still based on pure sinusoidal assumption. This problem motivates us to look for some new methods to reconstruct the 3-D profile based on non-sinusoidal fringe patterns.

In this paper, we present two approaches to FPP based on generalized analysis model, which are referred to as Inverse Function based Shift Estimation (IFSE) and Gradient-based Shift Estimation (GSE). Compared with existing FPP approaches, the proposed algorithms does not require any prior knowledge of projection systems and structures of projected fringe patterns. Meanwhile, the performances of these two methods are compared and discussed.

This paper is organized as follows. Section 2 introduces the principle of generalized analysis model. In Section 3 two algorithms are proposed for fringe pattern profilometry. In Section 4, simulations are utilized to demonstrate the improvement of these two methods and compare the performance between them. Section 5 concludes this paper.

2. PRINCIPLE OF GENERALIZED ANALYSIS MODEL

A schematic diagram of a typical FPP system is shown in Fig.1. For simplicity, we consider a cross section of the object surface for a given y coordinate. Hence, the inten-

sity of fringe patterns captured by CCD camera and the height distribution function can be expressed as a function with single variable x . Thus we use $s(x)$ and $d(x)$ to denote the intensity of the projected and deformed fringe pattern respectively and use $h(x)$ to represent the height distribution of the object surface.

In order to establish the relationship between $s(x)$ and $d(x)$, we consider a beam of light corresponding to a pixel of the fringe pattern, denoted as E_pCH in Fig.1. It is seen that the light beam is projected at point C and reflected back to the camera if the reference plane exists. When the reference plane is removed, the same beam will be projected onto point H and reflected to the camera via the point D. Assuming that the object surface and the reference plane have the same reflective characteristics, $s(x)$ at the location C should exhibit the same intensity as $d(x)$ does at the location D, because they originate from the same point of the fringe pattern created by the projector. Hence we have

$$d(x_d) = s(x_c) \quad (1)$$

where x_c and x_d are the coordinate locations of point C and point D respectively. We use u to denote the distance from C to D, that is

$$u = x_d - x_c \quad (2)$$

From Eq.(1) and Eq.(2), we have

$$d(x_d) = s(x_d - u) \quad (3)$$

Obviously, u varies with the height of the point H on the object surface.

Meanwhile, because triangles E_pHE_c and CHD are similar, we have

$$\frac{x_c - x_d}{-h(x_h)} = \frac{d_0}{l_0 - h(x_h)} \quad (4)$$

where x_h is the x coordinate of point H, l_0 is the distance between the camera and the reference plane and d_0 is the distance between the camera and the projector.

As point H and point D are on the same reflected beam from point H to the camera, point H will have the same x coordinate as point D does in captured images, which implies $x_h = x_d$. So Eq.(4) can be rewritten as

$$\frac{x_c - x_d}{-h(x_d)} = \frac{d_0}{l_0 - h(x_d)} \quad (5)$$

As defined in Eq.(2), Eq.(5) can be expressed as

$$\frac{-u}{-h(x_d)} = \frac{d_0}{l_0 - h(x_d)} \quad (6)$$

As the height distribution $h(x)$ is a function of x_d , u should also be a function of x_d . Then we have

$$u(x_d) = \frac{d_0 h(x_d)}{l_0 - h(x_d)} \quad (7)$$

Eq.(7) also can be written as

$$h(x_d) = \frac{l_0 u(x_d)}{d_0 + u(x_d)} \quad (8)$$

Therefore, Eq.(3) can be expressed as

$$d(x_d) = s(x_d - u(x_d)) \quad (9)$$

where $u(x_d)$ is given by Eq.(7).

As Eq.(8) and Eq.(9) should apply to arbitrary x_d , hence by letting $x_d = x$, we can simplify the mathematical expressions and derive a general model as follows:

$$d(x) = s(x - u(x)) \quad (10)$$

$$h(x) = \frac{l_0 u(x)}{d_0 + u(x)} \quad (11)$$

Eq.(10) reveals that the deformed signal $d(x)$ is a shifted version of $s(x)$, and the shift function $u(x)$ can be used to determine the object height distribution by Eq.(11).

It is interesting to note that by letting $s(x)$ be a cosinusoidal signal in Eq.(10), we can easily derive the conventional phase-modulation model. This implies that the conventional model is a special case of our proposed model.

3. ALGORITHMS OF SHIFT ESTIMATION

3.1. Inverse Function based Shift Estimation (IFSE)

A straightforward method to calculate the shift distribution is to use inverse function. We assume the projected signal function $r = s(t)$ is a monotonic function or it is monotonic in intervals of t , in which $s(t)$ has a unique inverse function. Denoting the inverse function of $s(t)$ as $s^{-1}(v)$, we have

$$s^{-1}(s(t)) = t \quad (12)$$

Therefore, if we apply the inverse function $s^{-1}(v)$ to deformed signal $d(t)$, we will have

$$s^{-1}(d(t)) = s^{-1}\{s[t - u(x)]\} = t - u(t) \quad (13)$$

which means that we can obtain the shift function $u(t)$ by

$$u(t) = t - s^{-1}(d(t)) \quad (14)$$

It is obvious that from Eq.(14), the shift distribution can be calculated based on the fringe pattern projected on the reference plane and the deformed fringe pattern on the surface of the object. The key to calculating the shift distribution is to obtain the inverse function $s^{-1}(v)$. A possible way is to employ polynomial curve fitting, which will consequentially introduce fitting errors. We use the mean square error to evaluate the curve fitting error, which is defined as:

$$e_f = E[(y_f(x) - y(x))^2] \quad (15)$$

where $E(w)$ is the operation of calculating the mean value of w , $y(x)$ are the data to be fitting and $y_f(x)$ are the values of the curve fitting results calculated by the approximate polynomial. The fitting error e_f will decrease with the increasing of the polynomial degree. Therefore, In order to determine the degree of polynomial used for curve fitting, we setup an upper bound of e_f in advance, and then we find out the minimum degree of polynomial which makes the curve fitting error e_f less than the upper bound

we have setup. Hence the procedure of surface reconstruction is as follows:

Step 1. Set an upper bound of curve fitting error, e_m , and initialize k , the degree of polynomial used for curve fitting. The initial value of k equals 1.

Step 2. Based on the captured fringe pattern on the reference plane, $s(t)$, work out j_k , a polynomial of degree k to approximate the inverse function $s^{-1}(v)$ in least squares sense. More detailedly, at first, we take the straight line $t = r$ as a symmetry axis to obtain a symmetrical curve of $s(t)$ in each monotonic interval, which actually is the curve of the inverse function $s^{-1}(v)$. And then, we make curve fitting to the obtained symmetrical curve and obtain the curve fitting result j_k . This process is equivalent to directly fitting the inverse function $s^{-1}(v)$ by regarding the value of $s(t)$ as the variable and t as the value of the inverse function, rather than obtaining an approximate polynomial of the original function $s(t)$ before fitting the inverse function $s^{-1}(v)$.

Step 3. By Eq.(15), calculate the curve fitting error when using j_k to approximate $s^{-1}(v)$, if the error is less than e_m , continue to do Step 4, otherwise, set $k = k + 1$ and return to Step 2.

Step 4. Based on the curve fitting result $s^{-1}(v) \approx j_k$, and the values of deformed signal $d(t)$, we calculate the shift function $u(t)$ by Eq.(14).

3.2. Gradient-based Shift Estimation (GSE)

Because the value of shift function $u(x)$ determines the height distribution $h(x)$, the height can be obtained if we have $u(x)$. Hence, we should track the values of shift function $u(x)$ for each point x by using $s(x)$ and $d(x)$. For this purpose, we use square error defined below as an objective function with respect to $\hat{u}(x)$ that denotes the estimation of $u(x)$ at point x :

$$e^2(\hat{u}(x)) = [d(x) - s(x - \hat{u}(x))]^2 \quad (16)$$

In order to minimize the error e^2 , we use gradient-based method to obtain the estimation of $\hat{u}(x)$ in an iterative way:

$$\hat{u}_{m+1} = \hat{u}_m - \eta \frac{de^2}{d\hat{u}} \Big|_{\hat{u}=\hat{u}_m} \quad (17)$$

where η is the learning rate. The gradient can be derived as:

$$\begin{aligned} \frac{de^2}{d\hat{u}} \Big|_{\hat{u}=\hat{u}_m} &= 2e \frac{de}{d\hat{u}} \Big|_{\hat{u}=\hat{u}_m} = -2e \frac{ds}{d\hat{u}} \Big|_{\hat{u}=\hat{u}_m} \\ &= -2e \frac{s(x - (\hat{u}_m + 1)) - s(x - (\hat{u}_m - 1))}{(\hat{u}_m + 1) - (\hat{u}_m - 1)} \\ &= -e[s(x - \hat{u}_m - 1) - s(x - \hat{u}_m + 1)] \\ &= -[d(x) - s(x - \hat{u}_m)] \times \\ &\quad [s(x - \hat{u}_m - 1) - s(x - \hat{u}_m + 1)] \end{aligned} \quad (18)$$

Substituting Eq.(18) into Eq.(17), we can have an iterative equation to calculate the estimation of the value of shift function $u(x)$ at each point x .

$$\hat{u}_{m+1}(x) = \hat{u}_m(x) + \eta [d(x) - s(x - \hat{u}_m(x))] \times [s(x - \hat{u}_m(x) - 1) - s(x - \hat{u}_m(x) + 1)] \quad (19)$$

For each point x , the iteration continues until convergence. In other words, if $|\hat{u}_{m+1} - \hat{u}_m|$ is less than a given lower bound, we can obtain an estimation of the value of $u(x)$ at point x , $\hat{u}(x) = \hat{u}_m(x)$. Considering the continuity of the profiles, we can use the converged value $\hat{u}(x)$ as the initial value for the next point $x+1$. i.e. let $\hat{u}_1(x+1) = \hat{u}(x)$ and then continue doing the iteration for the next point $x + 1$, so that faster convergence can be achieved.

4. SIMULATION RESULTS

Simulations have been performed to verify effectiveness of our proposed algorithms and compare the different performance between them. In our simulation, we use a paraboloid object surface whose diameter and maximum height are 200mm and 160mm respectively. the projected fringe pattern is generated from a cosinusoidal signal distorted by a nonlinear function given by:

$$s(g(x)) = 0.002g^2(x) + g(x) + C \quad (20)$$

where C is a constant which can be ignored as it does not effect on reconstruction results, and $g(x) = A \cos(2\pi f_0 x)$, where f_0 is the spatial frequency of the fringe pattern, which is assumed to be 0.001/mm. For the simplicity of calculation, the amplitude of the cosinusoidal signal $g(x)$ is assumed to be 100. Meanwhile, we assume l_0 and d_0 in Fig.1 equal to 5 meters and 2 meters respectively. The spatial resolution of the captured image is assumed to be 1 pixel/mm.

Substituting $g(x) = A \cos(2\pi f_0 x)$ into Eq.(20) and discarding DC component, we have:

$$s(x) = 100 \cos(2\pi f_0 x) + 10 \cos(2\pi \cdot (2f_0)x) \quad (21)$$

Note for the projected fringe pattern given by Eq.(21), the second order harmonic only has -20db of power compared with the fundamental component. Corresponding to Eq.(21), the deformed fringe pattern can be expressed as:[1, 2]

$$d(x) = 100 \cos(2\pi f_0 x + \phi(x)) + 10 \cos(2\pi \cdot (2f_0)x + 2\phi(x)) \quad (22)$$

where $\phi(x)$ is the phase shift caused by the object surface. From Eq.(21) and (22), we can reconstruct the surface by various algorithms. Comparative reconstruction results are shown in Fig.2, where dashed lines represent the true value of the height distribution of the object surface and solid lines denote the reconstruction results by using different methods. From Fig.2(a), it can be seen that nonlinear distortion introduces noticeable errors when PSP is used, even though the nonlinear distortion is so slight that coefficient of square item in Eq.(20) is only 0.002 and the second order harmonic only has -20db of power compared with fundamental component. Comparatively, by IFSE and GSE, we can have much better results shown in 2(b),(c) and (d). In Fig.2(b), the degree of polynomial is 8 and in Fig.2(c), it is 30. We can see that for IFSE, higher degree of the polynomial can have better reconstruction

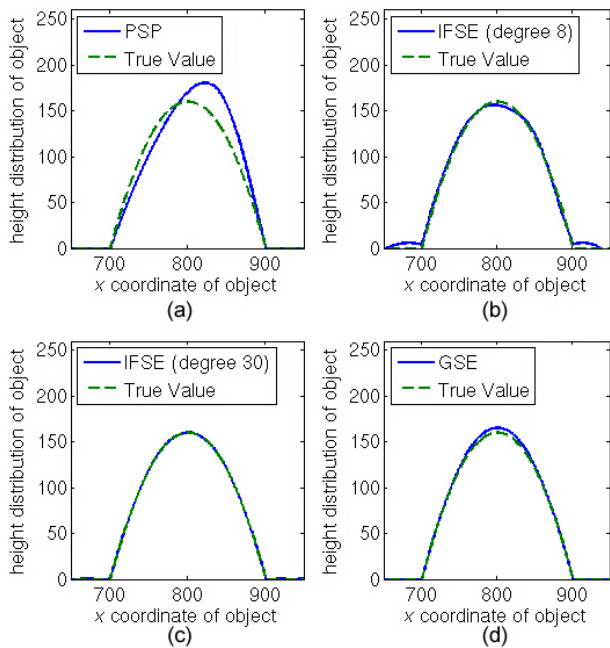


Fig. 2. Reconstruction results and error comparison

accuracy. In fact, theoretically, if the degree of polynomial is big enough, we always can have good reconstruction result. However, for big degrees, we need much more calculation time for curve fitting. i.e. the computation complexity of using IFSE depends on the polynomial degrees we are using. On the other hand, Fig.2(d) shows GSE also gives much improved measurement results compared with PSP. In a word, both of IFSE and GSE can obtain much better measurement accuracy than PSP when nonlinear distortion exists.

Further, in order to compare the performance between IFSE and GSE, Fig.3 shows the distribution of the measurement errors of reconstructed profile by using these two methods. In Fig.3, we can see that lower degree of

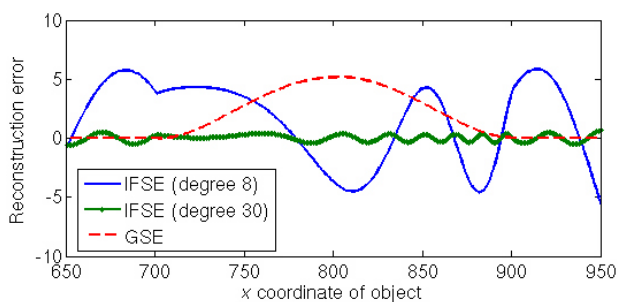


Fig. 3. Reconstruction results and error comparison

polynomial, which is 8 here, can not give reconstruction result as smooth as GSE does. In order to obtain smooth reconstruction results like GSE does, the degree of polynomial for IFSE has to be very high, which is 30 here. However, using higher degree of polynomial will cause much higher computation complexity.

5. CONCLUSION

In this paper, we have proposed two algorithms, IFSE and GSE, for fringe pattern profilometry, both of which can significantly improve the measurement accuracy. Even if the original signal is nonlinearly distorted, we can still obtain very accurate reconstruction results without any prior knowledge of the characteristics of the profilometry system. The effectiveness of our proposed algorithms have been confirmed by our simulation results. Meanwhile, according to our comparison between these two methods, it can be seen that the reconstruction accuracy of IFSE is much dependent on the degree of the polynomial for curve fitting. When lower degrees are used, IFSE can not reconstruct the object surface as precise as GSE does. In order to have accurate results as GSE, IFSE has to use higher degree polynomials, which will accordingly lead to higher computation complexity.

6. REFERENCES

- [1] Xianyu Su and Wenjing Chen, "Fourier transform profilometry: a review," *Optics and Lasers in Engineering*, vol. 35, pp. 263–284, 2001.
- [2] Xianyu Su, Wenjing Chen, Qichan Zhang, and Yiping Chao, "Dynamic 3-d shape measurement method based on ftp," *Optics and Lasers in Engineering*, vol. 36, pp. 49–64, 2001.
- [3] HJ Su, JL Li, and XY Su, "Phase algorithm without the influence of carrier frequency," *Optics Engineering*, vol. 36, pp. 1799–1805, 1997.
- [4] S Toyooka and Y Iwaasa, "Automatic profilometry of 3-d diffuse objects by spatial phase detection," *Applied Optics*, vol. 25, pp. 1630–1633, 1986.
- [5] R Rodriguez-Vera and M Servin, "Phase locked loop profilometry," *Optics and Lasers Technology*, vol. 26, pp. 393–398, 1994.
- [6] AJ Moore and F Mendoza-Santoyo, "Phase demodulation in the space domain without a fringe carrier," *Optics and Lasers in Engineering*, vol. 23, pp. 319–330, 1995.
- [7] J Villa, M Servin, and L Castillo, "Profilometry for the measurement of 3-d object shapes based on regularized filters," *Optics Communication*, vol. 161, pp. 13–18, 1999.
- [8] Lar Kinell, "Multichannel method for absolute shape measurement using projected fringes," *Optics and Lasers in Engineering*, vol. 41, pp. 57–71, 2004.
- [9] Yingsong Hu, Jiangtao Xi, Enbang Li, Joe Chicharo, Zongkai Yang, and Yanguang Yu, "A calibration approach for decoupling colour cross-talk using nonlinear blind signal separation network," in *IEEE Conference on Optoelectronic and Microelectronic Materials and Devices*, 2004.